Subcycle Fatigue Crack Growth Mechanism Investigation for Aluminum Alloys and Steels

Jian Yang[1], Wei Zhang[1], Yongming Liu[1,*]

[1] Mechanical Engineering, Arizona State University, Tempe 85281, US
* Corresponding author: yongming.liu@asu.edu

Abstract In this paper, the existence of crack closure and its sufficiency for crack growth prediction is investigated by multi-resolution in-situ optical microscopy experiment and SEM experiment. In in-situ optical microscopy testing, the digital image correlation analysis is used to measure the plastic zone size in front of the crack tip. In in-situ SEM testing, the crack tip opening displacement and the crack growth kinetics are investigated. Besides, crack closure behavior under constant loading with a single overload is studied in in-situ SEM test. This experimental methodology is applied to two different metallic materials (aluminum alloys and steels). Detailed imaging analysis and experimental results are presented and compared. It is found that first, there exists crack closure phenomena for aluminum alloys, but not for steels in our current researches; second, the crack closure will significantly change the crack tip plasticity behavior; third, the crack closure concept is able to account for crack growth kinetics uniquely for constant loading, but it is insufficient for constant loading with a single overload. Finally, the necessarily and the insufficiency of crack closure for crack growth prediction is discussed.

Keywords fatigue, crack closure, crack growth, plastic zone, overload

1. Introduction

In the past half century, many existing studies have been done on fatigue crack growth mechanism and prediction models. The most famous and successful model should be Paris' Law, which based on the applied stress intensity range [1]. However, Paris' model cannot be applied to loadings with different load ratio and modification is required. In 1970, Elber introduced a crack closure mechanism and modified the applied stress intensity factor range in order to characterize the effect of load ratio [2]. Since Elber's discovery provides a physical meaning to the modification, many researches have been done to get crack-opening load in theoretical method or experimental way. In 1978, Budiansky and Hutchinson provided an analytical estimation of crack opening load with the assumptions of long crack and small scale yielding according to the ideally plastic Dugdale-Barenblatt model [3]. In 1984, Newman analyzed the crack closure problems by developing a strip yield model, which employs a strip yield type plastic zone for leaving residually stretched material in the wake of the crack, causing plasticity-induced closure [4]. However, it is found that the measurement is difficult and the result depends on the measuring location and technique employed such as by traditional gauge and acoustic method [5]. Others methods like electrical potential method [6], ultrasonic method [7][8], and numerical method [9] are also used to measure crack opening load. These methods mentioned are indirectly way to observe crack closure and measure the crack opening loading, and it might be affected by many other factors, for example, it is found that commonly employed notch-mouth clip-gauge method is not sensitive enough to detect the closure of short cracks in regions of notch plasticity [10].

In this paper, in-situ testing and imaging analysis is used to directly observe the crack closure level and its relationship with crack tip behavior. Compare to the other indirect method, it is non-contact and can provide direct evidence about the crack closure at very different resolutions. Next, the proposed methodology is applied to two different metallic material systems and the existence of crack closure is investigated in detail. Following the testing under constant loading, a variable loading situation is tested to investigate crack closure effects on crack growth rate. In mechanics,

the crack closure behavior under overloading load is investigated in detail. Meanwhile, a statistical crack growth rate under constant loading and overloading load is compared. Finally, a discussion for the existence and insufficiency of crack closure for the fatigue crack growth analysis is given based on the current investigation.

2. In-situ optical microscopy study for crack closure

In in-situ optical microscopy test, a unit load cycle is divided into several steps and images are taken at each step. By digital image correlation analysis, then the strain distribution can be calculated. When the load is decreasing, the plastic zone is increasing due to the reversed plastic flow. However, if the crack is closed, the crack surfaces will contact and begin to undertake the reversed stress, thus the reversed plastic zone size will stop increasing. The reversed plastic zone size is a better indicator for crack closure than many other methods due to the advantages of non-contact and a stable precision inherited from digital image correlation method.

2.1. Experiment set-up and procedure

The experimental set-up for in-situ optical microscopy experiment is shown in Figure 1. It contains two parts: a palm-sized tensile stage and an optical microscope system. The tensile stage is fixed on the microscope and the cyclic loading is applied to the specimen. A Nikon metallurgical microscope is used to monitor the specimen surface and a high resolution imaging acquisition system is used to record images during the testing.

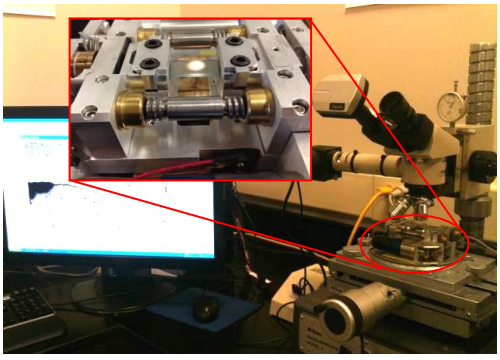

Figure 1. Experiment setup

The specimen is a ingle edge notched plate with width W = 8 mm, length L = 52 mm and thickness T = 0.86 mm. Due to the small thickness of specimens, it is assumed to be under the plane stress conditions for a relatively long crack. An edge notch of length 1mm is machined on the specimen. After machining, the specimens are pre-cracked until the initial crack reaches about 1 mm. The pre-cracking procedure follows the ASTM standard E647-08. Following this, both surfaces of the specimen are polished with the sandpaper whose average particle diameter is smaller than 10 um.

The experiment procedure contains four major steps.

Step 1: specimen manufacturing and pre-cracking. Single edge notched plate specimen is used for testing. After notching, the specimens are pre-cracked under a hydraulic tension machine INSTRON 1331 until the initial crack reaches about 1 mm. The pre-cracking procedure follows the ASTM standard E647-99;

Step 2: polish the specimen to form randomly distributed small dark regions on the smooth surface,

which is a requirement for digital image correlation (DIC) analysis. Both surfaces of the specimen should be polished with the sandpaper whose average particle diameter is smaller than 10 um. The final polishing is done using a vibration polishing machine with 1~3um polishing suspension;

Step 3: apply load on the specimen under the monitoring of a microscope, while image of the crack tip region is taken during the loading and unloading process. A unit load cycle is divided into several steps in the load profile. At each step, the image around the crack region is taken for strain calculation. The step load is set according to the precision requirement and computation resource limitation. An example profile is shown in Figure 2, which has about forty segments during the loading and unloading path.

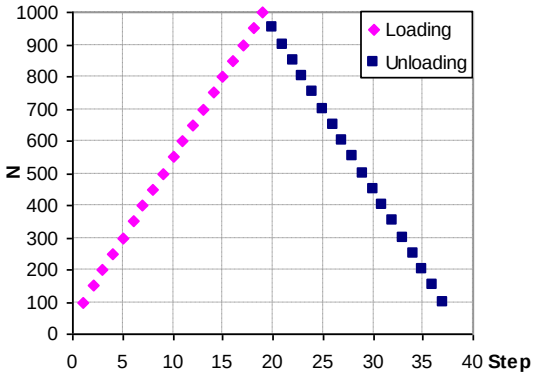

Figure 2. Load profile

Step 4, process the images by DIC software to get the strain field of the crack tip region and calculate the plastic zone using mechanical analysis. The plastic zone size is defined along the crack propagation direction and it can be measured directly from the processed image.

The theoretical reversed plastic zone under cyclic loading can be estimated by Eq. (1) without the consideration of crack closure [11]

$$\rho = \frac{1}{\pi}\left(\frac{\Delta K}{2\sigma_y}\right)^2, \tag{1}$$

where σ_y is the yielding strength and

$$\Delta K = F \cdot \Delta\sigma\sqrt{\pi a} = F \cdot (\sigma_{\max} - \sigma_{\min})\sqrt{\pi a} \tag{2}$$

where F is the geometry factor and

$$\mathrm{F} = 1.12 - 0.231\left(\frac{a}{W}\right) + 10.55\left(\frac{a}{W}\right)^2 - 21.72\left(\frac{a}{W}\right)^2 + 30.39\left(\frac{a}{W}\right)^3 \tag{3}$$

where a is the crack length.

2.2. Title and author information

With the above described experiment procedure, two sets of experiment are carried out to investigate the crack closure behavior under constant loading in Al 7075-T6 and Steel 4340 separately.

The chemical composition aluminum 7075-T6 is listed in Table 1. The aluminum is the balance in the total weight. The basic physical properties are listed in Table 2.

Following the above discussed general experiment methodology, the plastic zone size at each

loading step can be measured using the digital image correlation analysis. Three specimens have been tested and the reversed plastic zone size is shown in Figure 3. It can be found that there is a plat form when stress intensity factor (SIF) is less than about 3.5 MPa·m$^{0.5}$, which indicates the crack closes and the reversed stress is released by the surface contact.

Table 1. Chemical composition of Al 7075-T6 (weight, %)

Element	Zn	Mg	Cu	Fe	Si	Mn	Cr
Min	5.1	2.1	1.2	0	0	0	0.18
Max	6.1	2.9	2.0	0.5	0.4	0.3	0.28

Table 2. Basic mechanical properties of Al 7075-T6

Elastic Modulus /GPa	Yield Strength /MPa	Tensile Strength /MPa
71.7	502~516	573~582

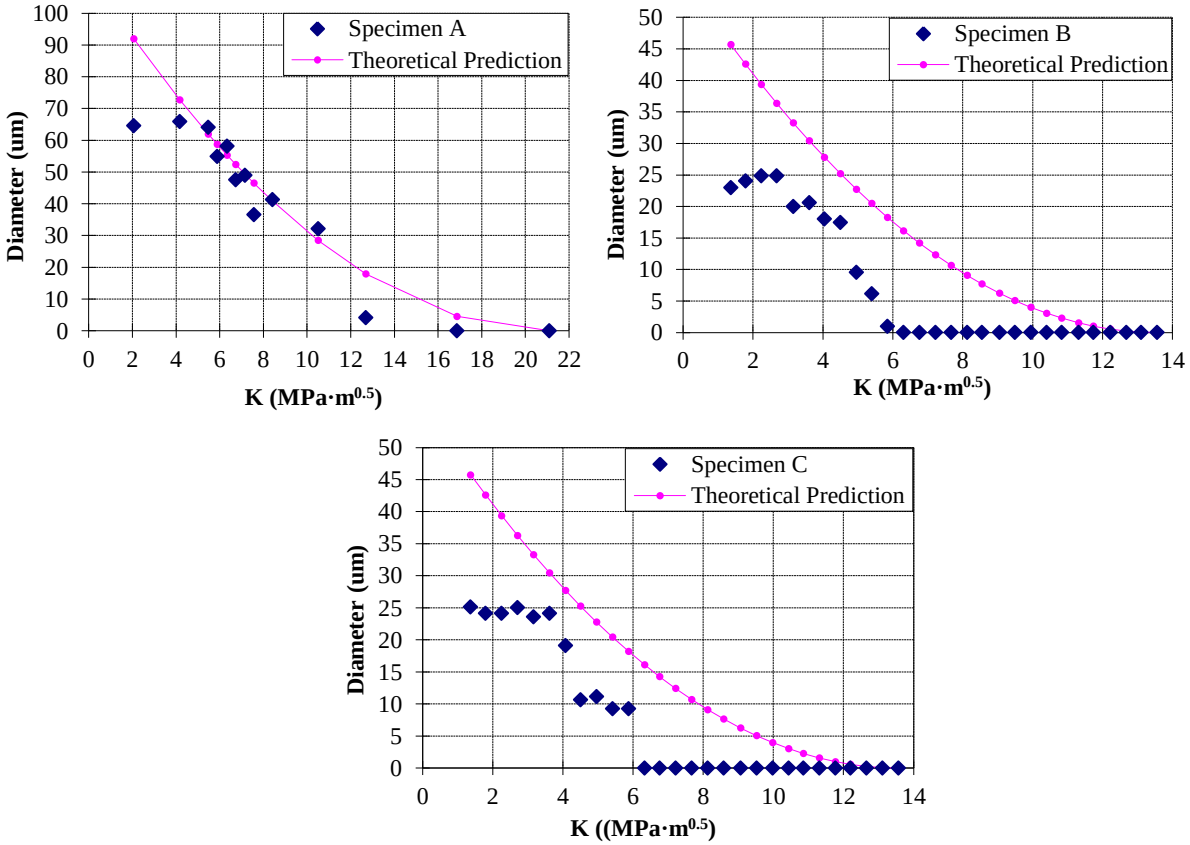

Figure 3. Plastic zone size of aluminum [12]

The same experiment is carried on steel 4340. AISI 4340 steel is a heat treatable, low alloy steel containing nickel, chromium and molybdenum. The chemical composition of this material and its basic physical properties are listed in Table 3 and 4.

Table 3. Chemical composition of AISI 4340 steel

Element	C	Cr	Mn	Mo	Ni	P	Si	S
Min	0.38	0.7	0.6	0.2	1.65	0	0.15	0
Max	0.43	0.9	0.8	0.3	2	0.035	0.3	0.04

Table 4. Basic physical properties of AISI 4340 steel

Elastic Modulus /GPa	Yield Strength /MPa	Tensile Strength /MPa
190~210	472.3	744.6

In the test, the load starts from 100 N to 1000 N at a step of 50 N. Result of the plastic zone size during the unloading process is obtained as shown in Figure 4. It is found that the reversed plastic zone size keeps increasing throughout the unloading process and these experiment data shows similar trends to the theory data without plastic closure phenomena. This is very different compared with the results of aluminum alloys and it indicates no crack closure for steel in these tests.

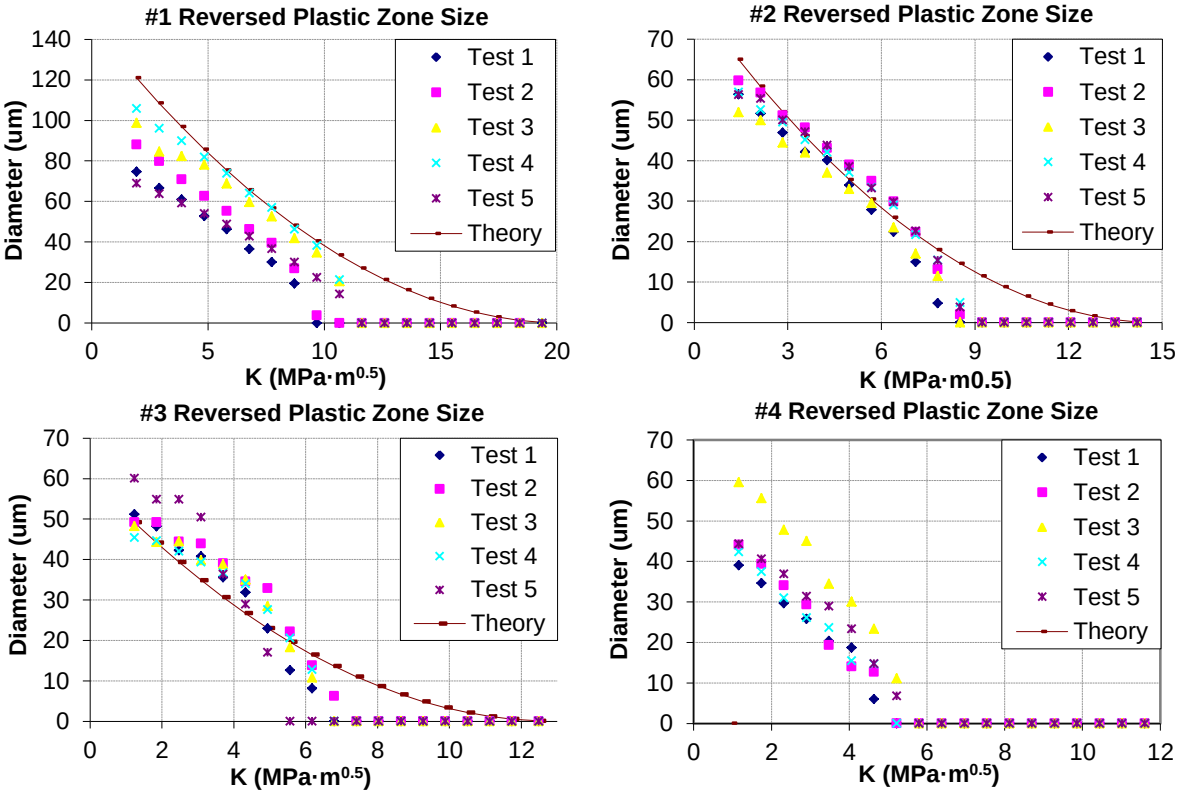

Figure 4. Plastic zone size of steel specimens

3. In-situ SEM study for crack closure

In order to verify the crack closure indications from optical microscope observation and get further information of the crack tip deformation behavior, in-situ SEM experiment is carried out on the two materials. Further, the behavior of crack closure under variable load is studied for the sufficiency of K_{eff} for crack growth prediction. In mechanics, crack closure behavior under a single overload is studied for the sufficiency of K_{eff} for crack propagation mechanics. In statistics, the crack growth rate under constant loading and overloading load is compared to show the sufficiency of K_{eff} for crack growth prediction. Detailed experimental procedure has been discussed in [13][14] and only a brief description of the experimental methodology is given below.

3.1. In-situ SEM study under constant amplitude loading

An in-situ SEM fatigue testing is performed to achieve the high resolution investigation for the hypothesis verification of crack growth kinetics and crack deformation in the vicinity of the crack tip. Compared with experiment under optical microscope, crack tip opening displacement (CTOD) is measured directly to find the crack is closed or not. Some details of the experimental set-up for the in-situ SEM experiment are shown in Figure 5. It consists of the tensile sub-stage and a field emission SEM (JEOL-7400F). The sub-stage is fixed in the SEM and the cyclic loading is applied during the experiment. Multiple resolution images are recorded during the testing for the

measurements of crack length and the crack tip deformation behavior.

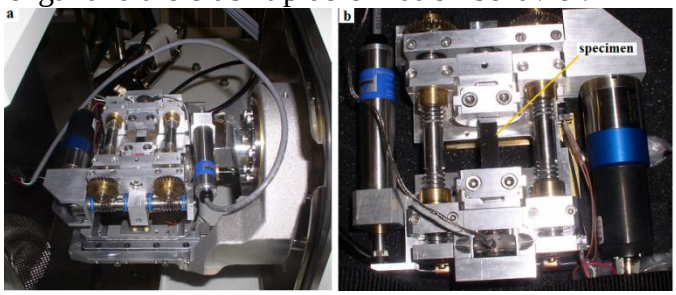

a) loading stage installed in SEM; b) specimen installed in loading stage.
Figure 5. In-situ SEM fatigue testing setup

The specimen configuration and preparation are almost the same as that in optical microscope experiment. In this experiment, the final polishing is done by a vibration polishing machine with 1~3 um polishing suspension.

The specimen is undergoing cyclic loading and observed in-situ under SEM. In the following comparison for aluminum and steel, the stress ratio is 0.1. The measurements are usually taken after 50 to 100 cycles to ensure the crack growth is stable. During the testing, one loading cycle is divided into many steps, similar with the testing under optical microscopy. The applied loading increases/decreases at a very slow rate. CTOD is measured directly from the processed images. The CTOD is defined as the distance of crack surface at the place of crack tip in last cycle. With the same reference, the crack growth rate at each cycle could be measured, as shown in Figure 6.

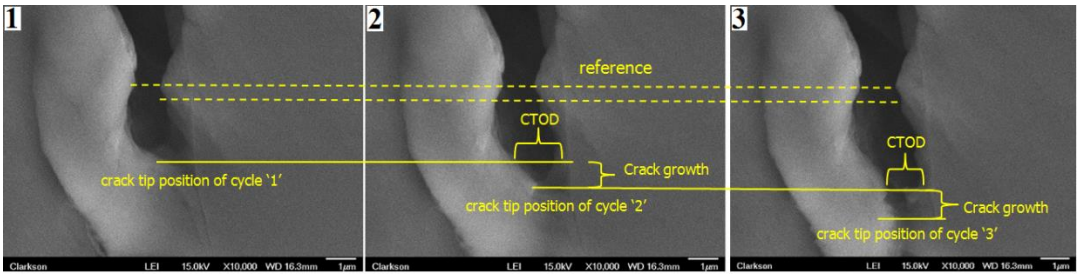

Figure 6. Images of crack tip position and CTOD under maximum loadings

Using the measuring method, two sets of experiments on steel 4043 and aluminum 7075-T6 have been performed. The results are shown in Figure 7. It shows that CTOD reduces to zero when SIF is less than 5 MPa·m$^{0.5}$ for Al 7075-T6, while for steel 4340, CTOD is not zero under the minimum loading. The crack tip details are shown in Figure 8. It shows the crack closure in Al 7075-T6 clearly but the crack remains open for steel 4340.

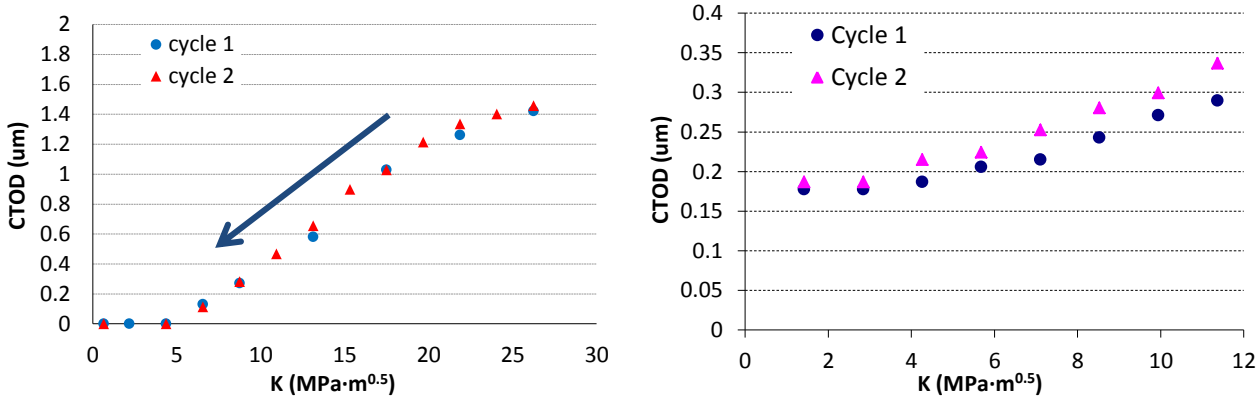

(a) Al 7075-T6 (b) Steel 4340

Figure 7. CTOD during unloading process on Al 7075-T6 and steel 4340

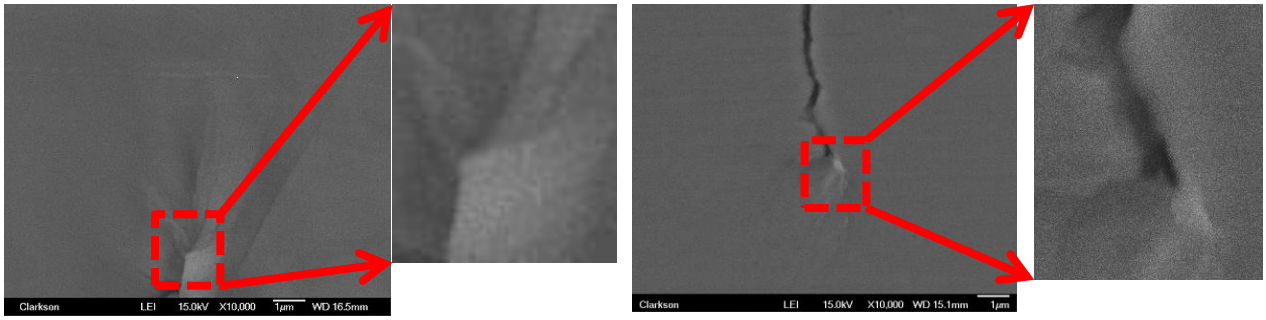

(a) Al 7075-T6 (b) Steel 4340

Figure 8. Crack tip under minimum loading of Al 7075-T6 and steel 4340

This result is consistent to the experiment under optical microscope and they show that the existence of crack closure in Al 7075-T6, but it is not observed in steel 4340 at this stage.

3.2. In-situ SEM study under variable loading with single overload

As crack closure is observed both under optical microscope and SEM, its effects on crack growth rate is not negligible for fatigue crack growth prediction for some metallic materials, if it happens. However, it is not clear that the crack closure is the only/dominant mechanisms for aluminum materials, especially under different loading conditions. Thus, the crack closure effect on crack growth rate under variable loading is investigated and is shown below.

The procedure of SEM experiment under variable loading is the same with that under constant loading. The only difference is the loading profile. In this experiment, a cycle of over-load is inserted in a constant loading spectrum. The constant loading ranges from 10 to 30 MPa·$m^{0.5}$ and the overload ranges from 10 to 36 MPa·$m^{0.5}$. Thus the over load ratio is 1.2 as the ratio of two maximum load. A schematic plot is shown in Figure 9.

In order to observe and compare the effects of overload loading, four types of loading cycle are chosen for observations. The first type is the constant loading cycles before the over load (cycle **A** in Figure 9), which provides the baseline information of the crack propagation kinematics. The second and the third type are the overload cycle (B) and the cycle right after it (C). The last type is the cycle 5~20 cycles after the overload (D). In this study, two experiments data are obtained. In the first experiment, the background stress ratio is 0.33 and the overload ratio is 1.2. In the second experiment, the background stress ratio is 0.025 and the overload ratio is 1.1. In the following discussion, the result of the first experiment will be discussed in detail and the second one will be given as a comparison.

Following the experiment procedure and the loading profile, the details of crack growing before, during, and after overload under SEM is obtained and compared.

For all testing measurements, the crack opening stress intensity factor at each observing cycle are plotted in Figure 10. The X axis is cycle number and Y axis is the ratio of crack opening SIF over the maximum SIF (K_{open}/K_{max}). It is shown that during the constant loading in stage 1 (cycle A), K_{open}/K_{max} is 0.57. In the overload cycle (B) and right after the overload cycle (C), the crack opening slightly decreases and increases to about 75% after more than 10 cycles (D). Another experiment has been performed with stress ratio R=0.025, the maximum SIF of the constant loading is 26.26 MPa·$m^{0.5}$ and the overload ratio 1.1. Very similar result is observed as shown in Figure 11.

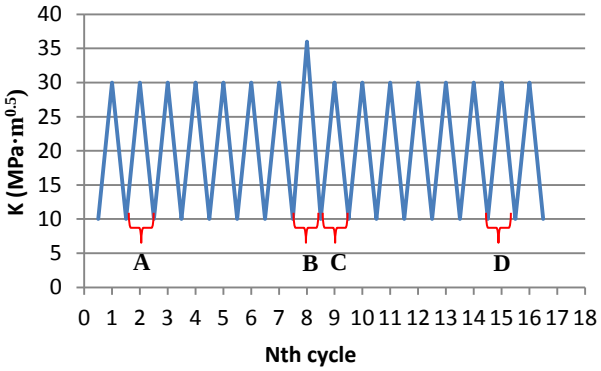

Figure 9. Schematic representation of single overload spectrum

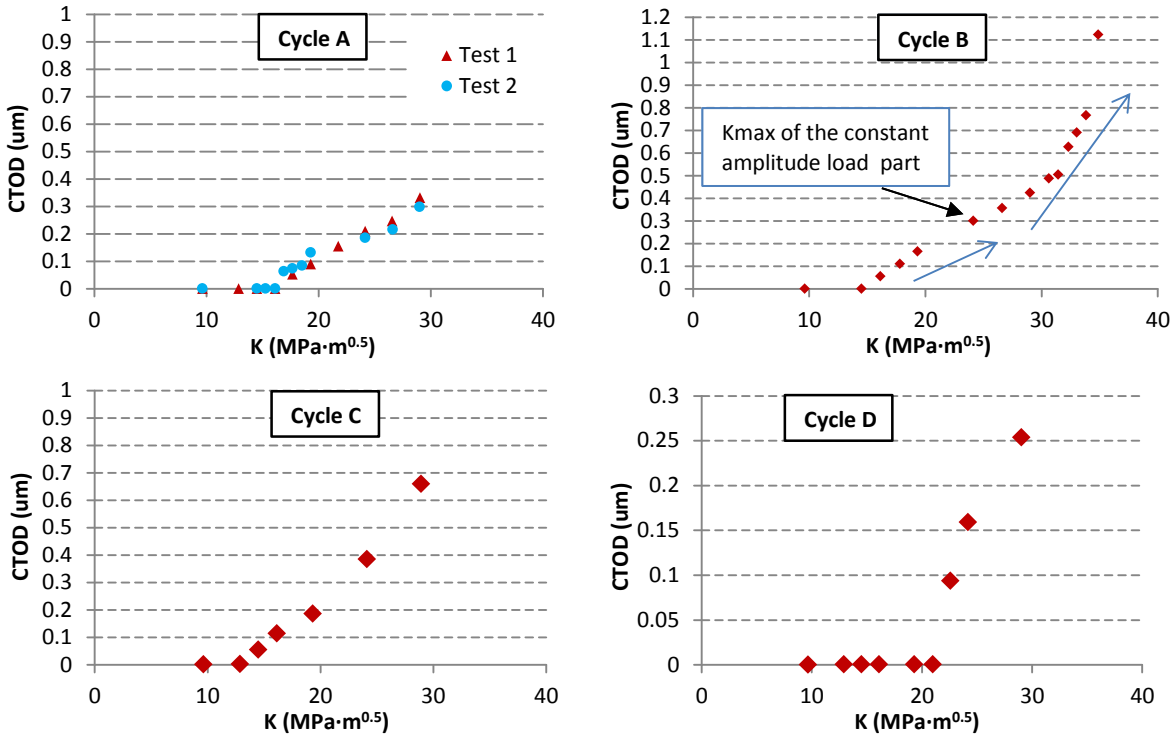

Figure 10. CTOD variation at each loading cycle in Figure 9

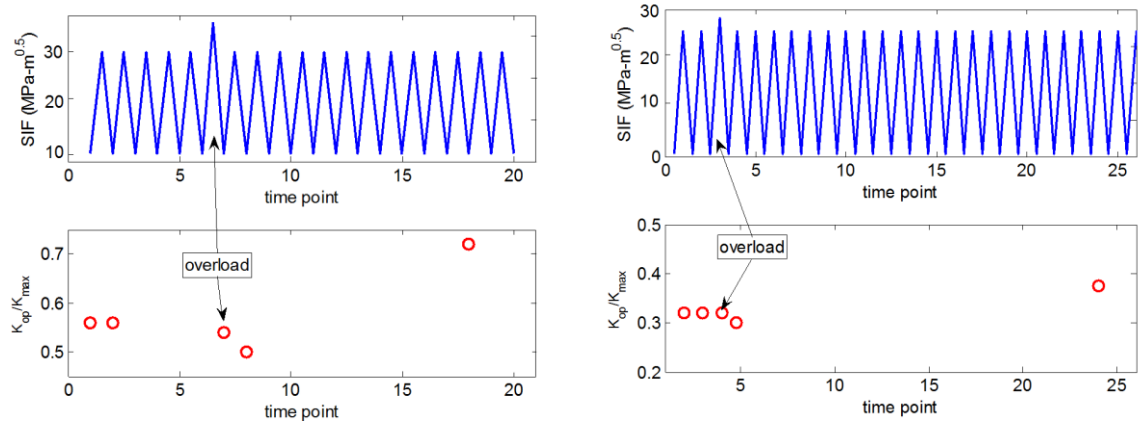

(a) R=0.33 (b) R=0.025

Figure 11. Illustration of the crack opening stress level variation

One important hypothesis in the classical crack closure theory is that the effective stress intensity

factor range (defined as the maximum SIF minus the opening SIF) can be used to uniquely correlate with crack growth rate under different loadings. However, this experiment shows that under single overload loading, crack opening SIF becomes variable and crack starts to kink and bifurcate. These mechanics cannot be explained only by the phenomena of crack closure.

Further, a statistical study of crack growth rate under constant load and overload lading is conducted to verify this hypothesis. Several experiments have been completed at stress ratio R=0.5, 0.33, 0.1 and 0.025, and the result of crack growth rate with the effective SIF is plotted in Figure 12. Figure 12 (a) shows the result under constant loading. It can be found that all the data shows a good linear relationship in log-log scale, except one data in red dashed circle. Figure 12(b) shows the data together with the single overload testing. It is observed that the two data points are not consistent with the linear trend from the constant amplitude loading data. This observation further indicates that other mechanism also contributes to the crack growth under single overload loading, such as crack branching and blunting as observed in the experiment.

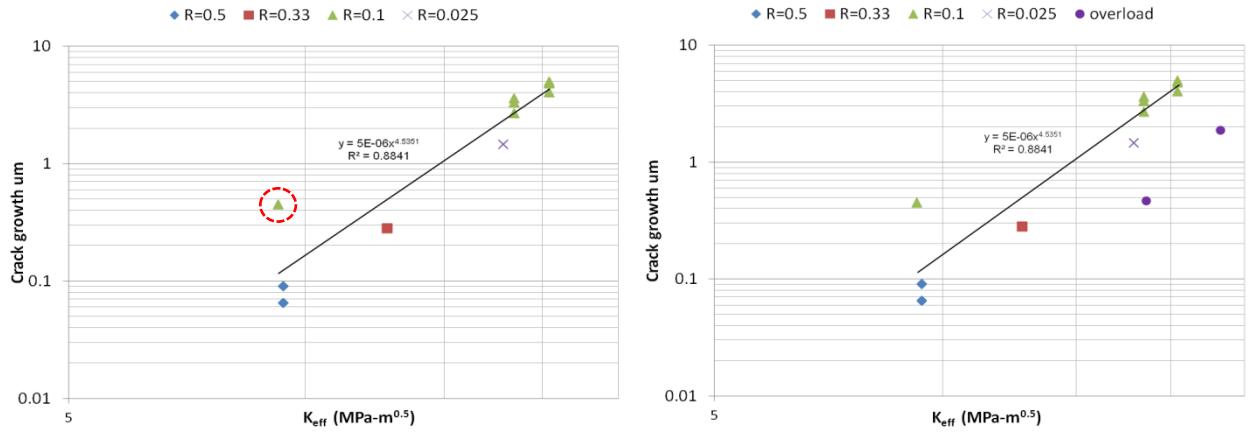

(a) Constant load (b) Constant loading and overloading load

Figure 12. Crack growth rate with SIF under constant load and overloading load

3. Conclusions

In this paper, in-situ experiment at micrometer scale and nanometer scale has been introduced and the observation of crack closure behavior of steel 4340 and aluminum 7075-T6 under constant loading has been obtained. Besides, preliminary crack closure behavior under single overload on aluminum 7075-T6 is studied. Several conclusions can be made from the experiments as follows.

1. Crack closure is directly observed in Al 7075-T6 under both constant and variable loads, but it is not observed in steel 4340 under constant loading at stress ratio 0.1.

2. The crack closure can significantly change the plasticity distribution in front of the crack tip;

3. K_{eff} defined as the difference of K_{max} and K_{open} in the classical fracture theory correlates with the unique crack growth rate under constant loading, but it not enough for crack growth prediction under variable loading. Additional parameter for the mechanism is need for the prediction;

The proposed study focus on simple variable loadings and more complex loading conditions require additional study. The current imaging analysis is for surface measurements and 3D imaging technique will be very helpful for the investigation of subsurface behavior near a crack tip.

Acknowledgements

The research was supported by funds from Air Force Office of Scientific Research: Young Investigator Program (Contract No. FA9550-11-1-0025, Project Manager: Dr. David Stargel). The support is gratefully acknowledged.

References

[1] P.C. Paris, M.P. Gomez, W.E. Anderson, A Rational Analytic Theory of Fatigue, Trend in Engineering. 13 (1961) 9–14.

[2] E. Wolf, Fatigue crack closure under cyclic tension, Engineering Fracture Mechanics. 2 (1970) 37–45.

[3] B. Budiansky, J. Hutchinson, Analysis of closure in fatigue crack growth, Journal of Applied Mechanics. 45 (1978) 267–276.

[4] J. J.C. Newman, A crack opening stress equation for fatigue crack growth, International Journal of Fracture. 24 (1984) R131–R135.

[5] D.E. Macha, D.M. Corbly, J.W. Jones, On the variation of fatigue-crack-opening load with measurement location, Experimental Mechanics. 19 (1979) 207–213.

[6] T.T. Shih, R.P. Wei, A study of crack closure in fatigue, Engineering Fracture Mechanics. 6 (1974) 19–32.

[7] D. Bouami, D. De Vadder, Detection and measurement of crack closure and opening by an ultrasonic method, Engineering Fracture Mechanics. 23 (1986) 913–920.

[8] D.S. Singh, A. Srivastav, S. Gupta, E. Keller, A. Ray, Ultrasonic measurement of crack opening load for life-extending control of mechanical structures, in: 2009 American Control Conference, IEEE, Piscataway, NJ, USA, 2009: pp. 210–215.

[9] W. Riddell, R. Piascik, M. Sutton, W. Zhao, S. McNeill, J. Helm, Determining Fatigue Crack Opening Loads from Near-Crack Tip Displacement Measurements, ASTM SPECIAL TECHNICAL PUBLICATION. 1343 (1999) 157–174.

[10] N. Fleck, C. Shin, Fatigue crack growth under compressive loading, Engineering Fracture Mechanics. 21 (1985) 173–185.

[11] J. Rice, A path independent integral and the approximate analysis of strain concentration by notches and cracks, Journal of Applied Mechanics. 35 (1968) 379–386.

[12] W. Zhang, Y. Liu, Plastic zone size estimation under cyclic loadings using in situ optical microscopy fatigue testing, Fatigue & Fracture of Engineering Materials & Structures. 34 (2011) 717–727.

[13] W. Zhang, Y. Liu, Investigation of incremental fatigue crack growth mechanisms using in situ SEM testing, International Journal of Fatigue. 42 (2012) 14–23.

[14] W. Zhang, Y. Liu, In situ SEM testing for crack closure investigation and virtual crack annealing model development, International Journal of Fatigue. 43 (2012) 188–196.